JMEPEG (2015) 24:4322–4327
DOI: 10.1007/s11665-015-1722-8

1059-9495/$19.00

Effect of Surplus Phase on the Microstructure and Mechanical Properties in Al-Cu-Mg-Ag Alloys with High Cu/Mg Ratio

Xiaofeng Xu, Yuguang Zhao, Xudong Wang, Ming Zhang, and Yuheng Ning

(Submitted July 18, 2015; in revised form August 30, 2015; published online September 28, 2015)

In order to examine the effect of surplus phase on the microstructure and mechanical properties, different compositions with high Cu/Mg ratio of the T6-temper extruded Al-Cu-Mg-Ag alloys were studied in this investigation. The results show that the Al-5.6Cu-0.56Mg-0.4Ag alloy obtains superior mechanical properties at room temperature, while the yield strength of Al-6.3Cu-0.48Mg-0.4Ag alloy is 378 MPa at 200 °C, which is 200 MPa higher than that of Al-5.6Cu-0.56Mg-0.4Ag alloy. Although the excessive Cu content causes the slight strength loss and elongation decrease in the Al-6.3Cu-0.48Mg-0.4Ag alloy at room temperature, the surplus phases and recrystallized microstructure will play an effective role in strengthening the alloy at elevated temperature.

Keywords mechanical properties, metals and alloys, microstructure, recrystallization, surplus phase

1. Introduction

The precipitation hardened Al-Cu-Mg-Ag alloy exhibits certain excellent properties, such as high strength and good creep resistance, due to the formation of the fine and uniform distribution precipitate Ω (Ref 1-3). As a result, these alloys are considered to be commercially available and currently being developed as potential materials for future applications in the aerospace industry (Ref 4, 5).

In the past decades, the Al-Cu-Mg-Ag alloys with various compositions are designed and studied; the study is helpful for understanding the effect of element content on the microstructure and mechanical properties in the alloys. For example, several studies indicated that increasing the Ag content from 0.4 to 0.8 wt.% had few effects on the enhancement of the Ω phase precipitation (Ref 6, 7). While Zhou et al. (Ref 8) reported that the age-hardening response and mechanical properties of the Al-Cu-Mg alloys were enhanced as the Ag content increased from 0.14 to 0.57 wt.%. Besides, the alloy system with high Cu:Mg ratios is proved to be beneficial for the precipitation of Ω phase (Ref 9). However, due to the important role of Mg in the precipitation of Ω phase, the Cu:Mg ratios are often adjusted through changing the Cu content (Ref 6, 10). In addition, when the Mg content remained the same, with increasing the Cu content, the strength of the alloy was improved, whereas the elongation decreased (Ref 11), and the changed Mg content made the similar trend when the Cu content stayed unchanged (Ref 12). As a result, the appropriate Cu and Mg content plays a key role in obtaining the superior mechanical properties in the alloy.

As is known, the solid solution limit of Cu in Al is 5.6 wt.% at 548 °C, therefore, when the Cu content exceeds the largest solubility, there are residual phases after solid solution treatment (SST). Although the surplus phases can strengthen the alloys, the nonuniform coarse phases have a remarkably negative effect on the elongation of the alloy (Ref 13). However, as a severe plastic deformation method, hot extrusion can make the elements uniform and compact the alloy, moreover, the secondary phases will distribute uniformly in the matrix after the hot extruding, which will be beneficial for improving the ductility in the alloy (Ref 14, 15). Nevertheless, most of the studies focus on the effect of the precipitates on the microstructure and mechanical properties in the Al-Cu-Mg-Ag alloy. There are few studies about the influence of surplus phases on the precipitation and mechanical behavior of the alloy. Based on the problems above, the Al-Cu-Mg-Ag alloy will be studied in this paper.

2. Experimental

The experimental material Al-Cu-Mg-Ag alloys were prepared with pure Al, pure Cu, pure Mg, pure Ag and Al-5Zr, Al-15Mn, Al-5Ti-B master alloys by ingot metallurgy in a crucible furnace. The nominal compositions of the alloys are shown in Table 1. After casting, the ingot rods were homogenized at 500 °C for 24 h, processed to 80 mm and then extruded to 8 mm thin plate with the extrusion ratio of 16.5 at about 400 °C, then cooled in the air. To obtain the optimized solid solution temperature, the dissolving temperature of secondary phases of the extruded samples was determined using differential scanning calorimetry (DSC) at heating rate of 10 °C/min. Vickers microhardness was measured with a load of 50 g for a holding time of 10 s. At least 10 points were measured for each sample. The tensile specimens were got parallel to the extruding direction, and at least 3 specimens were tested for

Xiaofeng Xu, Yuguang Zhao, Xudong Wang, Ming Zhang, and **Yuheng Ning**, Key Laboratory of Automobile Materials, Ministry of Education, and Department of Materials Science and Engineering, Jilin University, No. 5988 Renmin Street, Changchun 130025, People's Republic of China. Contact e-mail: zhaoyg@jlu.edu.cn.

Table 1 Nominal compositions of the alloys investigated (wt.%)

Alloy	Cu	Mg	Ag	Zr	Mn	Ti	Fe	Si	Al
1	4.8	0.6	0.4	0.2	0.3	<0.1	<0.1	<0.05	Bal.
2	5.6	0.56	0.4	0.2	0.3	<0.1	<0.1	<0.05	Bal.
3	6.3	0.48	0.4	0.2	0.3	<0.1	<0.1	<0.05	Bal.

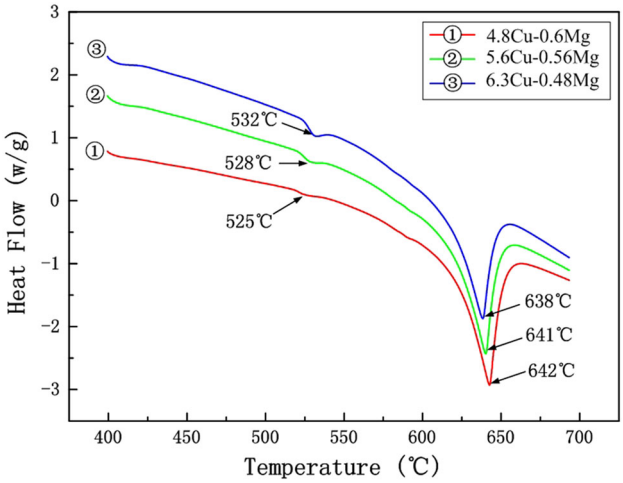

Fig. 1 DSC curves of extruded Al-Cu-Mg-Ag alloys with different compositions

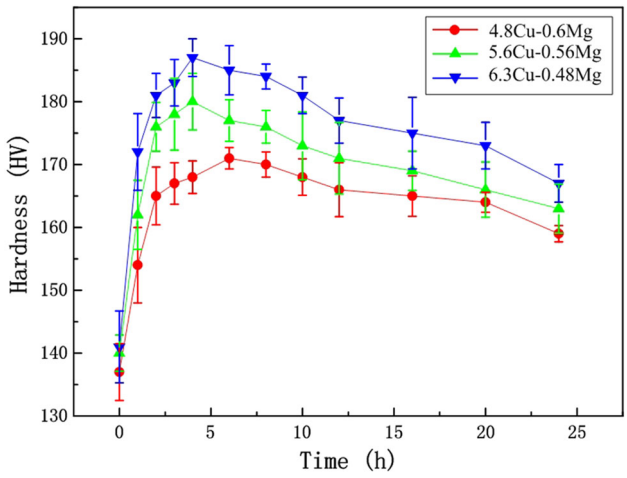

Fig. 2 Hardness vs. aging time at 185 °C

each condition. Tensile tests were carried out at a strain rate of 10^{-3} s^{-1} at room and elevated temperature. Microstructure characterizations were performed on optical microscope (Carl Zeiss Axio Imager A2m, Germany). The specimens for transmission electron microscope (TEM) observation were prepared by the standard twin-jet electropolishing method with a voltage of 10-15 V in 80% ethanol and 20% perchloric acid at −30 °C. The TEM observations were carried out on a JEM-2100F and operated at 200 kV.

3. Results and Discussion

Figure 1 presents the DSC traces of the alloys after hot extrusion. Two exothermal peaks are apparent in each DSC thermogram, and the first peak indicates the dissolving reactions of the secondary phase. The solution temperature indicates a slight increasing trend with improving the Cu content. It should be noted that the dissolving temperature of the second-phase can be reduced by the alloying elements. To ensure the second-phase having enough time to dissolve in the matrix, the solid solution time was confirmed as 2 h. On account of the dissolving temperature of secondary phase and avoiding the alloy overburning, the solid-solution temperatures are optimized as (the optimized process was not shown): 515 °C (4.8Cu-0.6Mg Alloy), 515 °C (5.6Cu-0.56Mg Alloy), and 520 °C (6.3Cu-0.48Mg Alloy). The specimens were solid solution treated, subsequently water quenched and then immediately aged at 185 °C for up to 24 h (T6 temper).

Figure 2 shows the evolution of Vickers microhardness as a function of aging time for the Al alloy samples with different compositions. The 4.8Cu-0.6Mg alloy reaches its age-hardening peak of 170 after 6 h at an aging temperature of 185 °C, and further increasing the aging time results in a decrease in microhardness, indicating the occurrence of over-aging of the SST sample. While the other alloys reach the peak hardness after only 4 h. It can be concluded that the higher Cu content makes the more rapid age hardening and higher hardness, moreover, the peak aging time is confirmed as 6 h in 4.8Cu-0.6Mg alloy and 4 h for other alloys. The optimized T6 treatment parameters are shown in Table 2.

Table 2 The optimized T6 heat-treatment alloys with different compositions

Alloy	The SST temperature, °C	The peak-aged time at 185 °C, h
1	515	6
2	515	4
3	520	4

Based on the microhardness measurements, tensile tests were performed in order to better understand the mechanical performance of the aged alloys. Figure 3(a) shows the typical engineering stress-strain curves of the peak-aged alloys with various compositions. Although 4.8Cu-0.6Mg alloy has the slightly higher yield strength (YS), the ultimate tensile strength (UTS) and elongation of 5.6Cu-0.56Mg alloy (516 MPa and 17.4%) are both improved compared with 4.8Cu-0.6Mg alloy, when the Cu content was improved, the strength (YS and UTS) and elongation of 6.3Cu-0.48Mg alloy slightly decreases compared with 5.6Cu-0.56Mg alloy. As shown in Fig. 3a, 5.6Cu-0.56Mg alloy and 6.3Cu-0.48Mg alloy have better mechanical properties, and there are small differences between the two alloys. As a result, the mechanical behavior of the two

alloys was tested at elevated temperatures, as shown in Fig. 3(b). It can be seen that the high-temperature strength of the samples decreases and the elongation increases compared with that of room temperature. Although the 5.6Cu-0.56Mg alloy has slightly better mechanical behavior at room temperature, the 6.3Cu-0.48Mg alloy has higher YS (378 MPa) at elevated temperature, which is ~200 MPa higher than that of 5.6Cu-0.56Mg alloy.

Figure 4 shows the tensiled fracture surfaces of aged Al-Cu-Mg-Ag alloys at room temperature. There are many dimples with different size and shapes in every fracture, which is an indication that most of the failure is the result of ductile fracture. In particular, the dimples are formed around some residual particles. During deformation, some voids generally form around the interface of the secondary particles and the matrix. And with the deformation proceeding, the voids grow and some aggregate, providing the fracture sources (Ref 16). There are more dimples in Fig. 4(b) compared with that in Fig. 4(a), and the particles and the dimples are smaller in Fig. 4(b) than that in Fig. 4(c). So the elongation of the 5.6Cu-0.56Mg alloy is larger than that of the samples. It is in good accordance with the results of Fig. 3(a).

Figure 5 is the optical images showing the microstructure of the SST samples with different compositions, and as is known, the aging process has few effects on the optical image of the microstructure. The dispersed particles are identified as θ-phase dispersoids (Al_2Cu) by scanning electron microscopy (SEM) and energy dispersive x-ray (EDX) (Fig. 5d and e). As shown in Fig. 5, there are few residual phases in 4.8Cu-0.6Mg alloy after SST, and with increasing the Cu content, the residual phases increase both in the size and the volume fraction, moreover, the residual phases dispersed uniformly after extrusion and heat-treatment. Although the Cu content of 5.6Cu-0.56Mg alloy is just 5.6 wt.%, the other alloy elements make the Cu element hard to dissolve in the matrix totally. During SST, the elevated temperature accelerates the recovery and

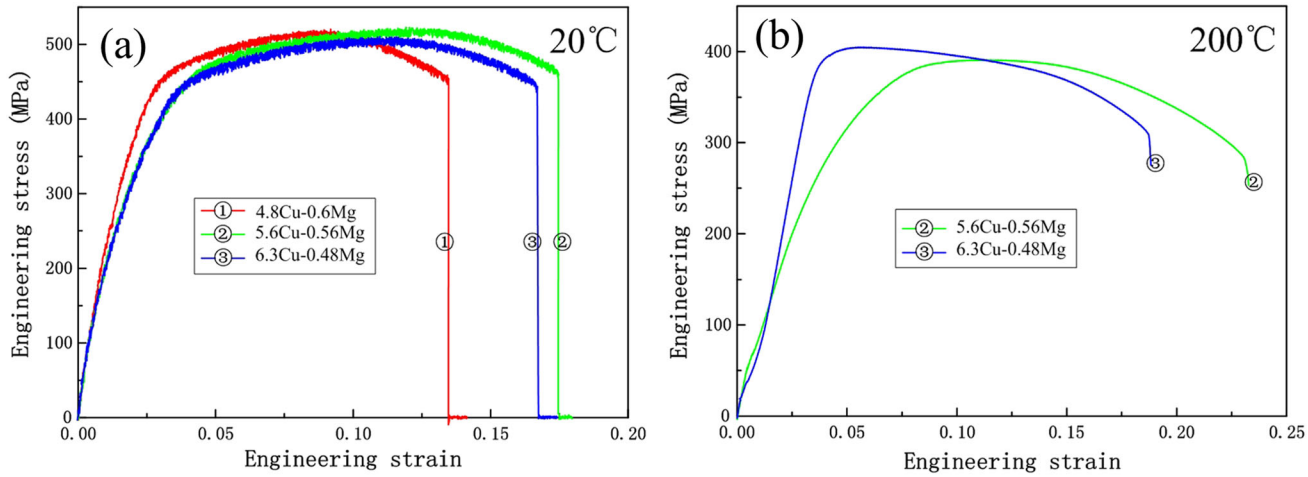

Fig. 3 Typical engineering stress-strain curves in the peak-aged conditions with various compositions: (a) at room temperature (20 °C) and (b) elevated temperature (200 °C)

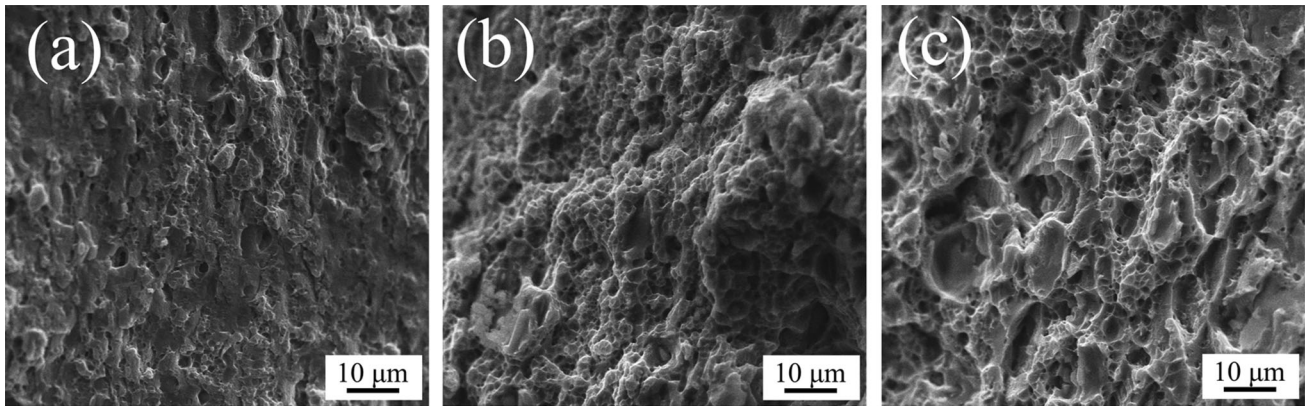

Fig. 4 Fracture surfaces of aged Al-Cu-Mg-Ag alloys with different compositions: (a) 4.8Cu-0.6Mg Alloy, (b) 5.6Cu-0.56Mg Alloy and (c) 6.3Cu-0.48Mg Alloy

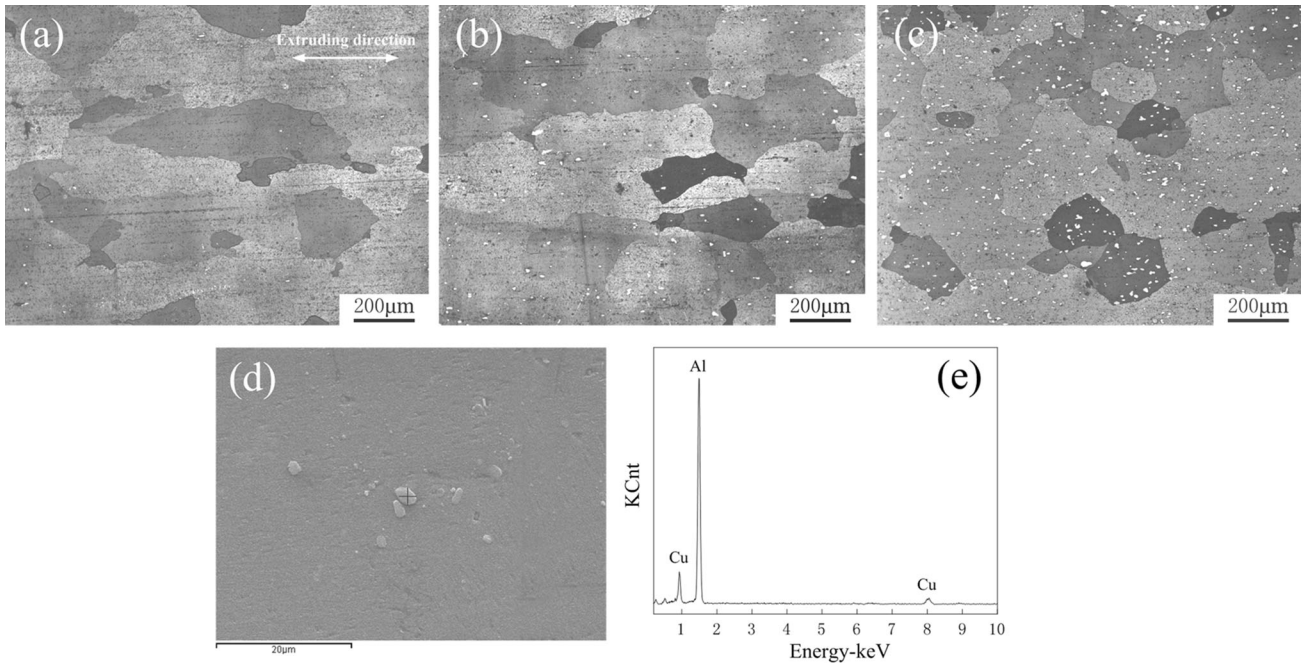

Fig. 5 Optical microstructures of the solution treated Al-Cu-Mg-Ag alloys with composition of (a) 4.8Cu-0.6Mg Alloy, (b) 5.6Cu-0.56Mg Alloy and (c) 6.3Cu-0.48Mg Alloy; (d) SEM and (e) EDX of the secondary phase in (c)

recrystallization of the alloys, and the surplus phases will serve as the core of the new grains, as a result, the higher Cu content alloy has the larger degree of recrystallization, which is beneficial for the stability of the alloy at elevated temperature (Ref 12). Although the recrystallized structure will provide more mobile slip systems to improve the plasticity, it also should be indicated that the surplus particles have a negative effect on the elongation of the samples during deformation. However, the surplus phases can be the obstacle for the motion of grain boundaries and dislocations (Ref 17), moreover, the high temperature has fewer effects on the growth of the coarse surplus phases compared with that of precipitates, therefore, the strength of 6.3Cu-0.48 Mg alloy is improved at elevated temperature, as shown in Fig. 3b, meanwhile, it should be noted that the uniformly dispersed surplus phase also has contribution to the hardness of the alloy (Fig. 2).

The TEM micrographs of the aged alloys with different compositions are shown in Fig. 6. The primary second-phases are plate-like Ω phase. For the plate-like Ω phase on the {111} planes, the increase in strength can be given by the relation (Ref 18): $\Delta\sigma = \frac{\Gamma}{r}\ln\left(\frac{0.158r}{r_0}\right)$, where $\Delta\sigma$ is the strength increase, r is the radius of the plate-plane, r_0 is the dislocations bypassing radius, Γ is the parameter only concerning to the volume fraction of the precipitation. In the same alloy system, it has been concluded that the smaller r and higher Γ make the larger $\Delta\sigma$. Due to the lower Cu content of 4.8Cu-0.6Mg alloy compared with other alloys, the driving force of precipitation will be lower after SST (Ref 6). However, the higher Mg content can provide more nucleation site (Ref 19, 20), and the longer aging time increases the volume fraction of precipitates, which doesn't induce the number of secondary phases decreasing distinctly, as shown in Fig. 6(a). Although the Mg-Ag clusters can be beneficial for precipitation and strengthening, they may affect the motion of dislocations during deformation (Ref 6), so the elongation decreases in 4.8Cu-0.6Mg alloy. While with increasing the Cu content, the degree of the supersaturation is enhanced after SST. When the Cu content exceeds the largest solubility (5.6 wt.%), the alloys present the nearly same precipitation. However, the surplus phases may serve as the core of the precipitates during age treatment, which partially weakens the dispersed effect of precipitation strengthening. Hence, it can be seen that 6.3Cu-0.48Mg alloy has the slightly smaller amount of precipitates compared with 5.6Cu-0.56Mg alloy, as shown in Fig. 6(b) and (c). As a result, the slightly decreased strength of 6.3Cu-0.48Mg alloy is the combined effects of the surplus phase strengthening and weakened precipitation strengthening.

4. Conclusions

Investigation on the influence of various compositions on the microstructure and mechanical properties of age hardened Al-Cu-Mg-Ag alloys was performed. The results show that increasing the Cu content can acquire higher hardness and accelerate the age-hardening response of the alloys. To obtain the super mechanical properties at room temperature, the Cu content should be controlled at about 0.56 wt.% in the alloy. The surplus phases will weaken the precipitation strengthening and promote the recrystallization during heat-treatment process. Although the excessive Cu content is slightly unbeneficial for the mechanical behavior at room temperature, the surplus phases will play an effective role in strengthening the Al-Cu-Mg-Ag alloy at elevated temperature.

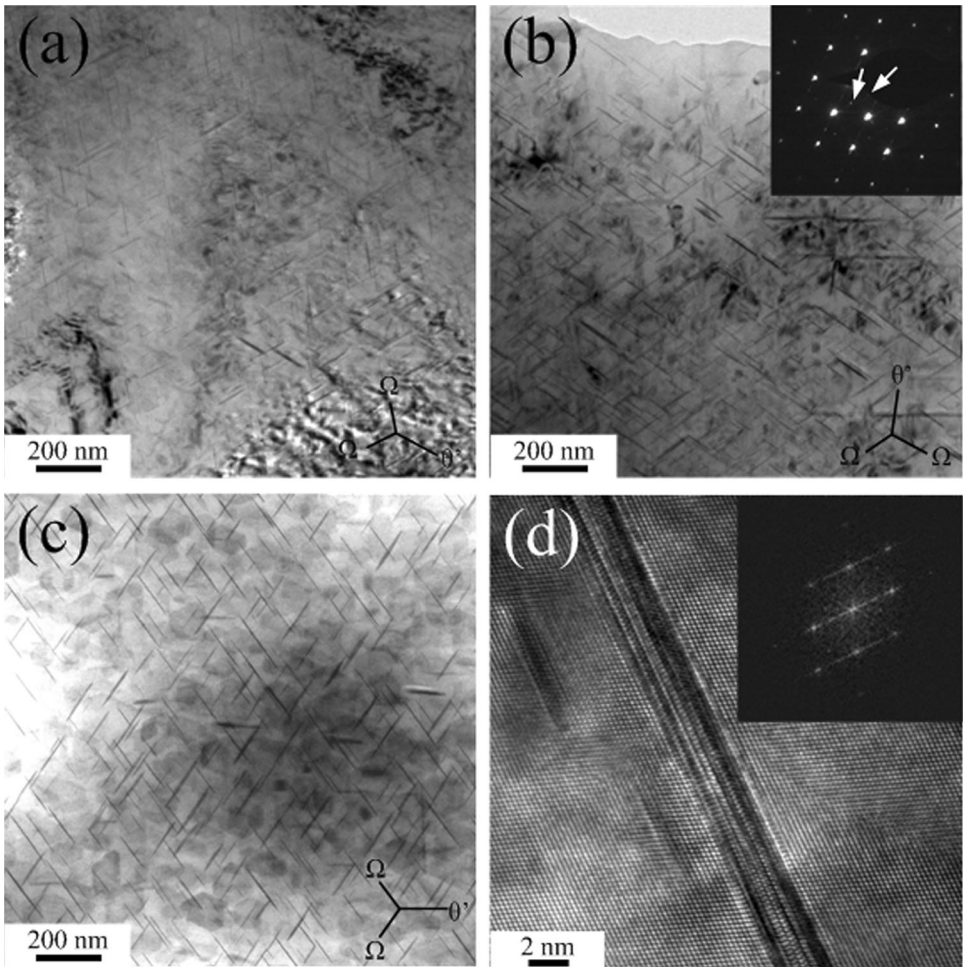

Fig. 6 Bright field TEM micrographs showing the microstructures with composition of (a) 4.8Cu-0.6Mg Alloy, (b) 5.6Cu-0.56Mg Alloy and (c) 6.3Cu-0.48Mg Alloy in peak-aged conditions; (d) high resolution transmission electron microscopy (HRTEM) and fast Fourier transformation (FFT) of the typical Ω phase in (c)

Acknowledgments

This work was supported by The National Natural Science Foundation of China (No. 51071075) and The Deep Continental Scientific Drilling Equipment Development (SinoProbe-09-05), as well as by The 985 Project-Automotive Engineering of Jilin University.

References

1. X.Y. Liu, Q.L. Pan, X.L. Zhang, S.X. Liang, F. Gao, L.Y. Zheng, and M.X. Li, Creep Behavior and Microstructural Evolution of Deformed Al-Cu-Mg-Ag Heat Resistant Alloy, *Mater. Sci. Eng. A*, 2014, **599**, p 160–165
2. C.R. Hutchinson, X. Fan, S.J. Pennycook, and G.J. Shiflet, On the Origin of the High Coarsening Resistance of Omega Plates in Al-Cu-Mg-Ag Alloys, *Acta Mater.*, 2001, **49**, p 2827–2841
3. J.B. Zhang, Y.A. Zhang, B.H. Zhu, R.Q. Liu, F. Wang, and Q.M. Liang, Characterization of Microstructure and Mechanical Properties of Al-Cu-Mg-Ag-(Mn/Zr) Alloy with High Cu:Mg, *Mater. Des.*, 2013, **49**, p 311–317
4. J.B. Zhang, Y.A. Zhang, B.H. Zhu, F. Wang, Z.H. Li, X.W. Li, and B.Q. Xiong, Identification of Thermal Effects Involved in DSC Experiment on Al-Cu-Mg-Ag Alloys with High Cu:Mg Ratio, *Int. J. Miner. Metall. Mater.*, 2011, **18**, p 671–675
5. S. Bai, Z.Y. Liu, Y.T. Lia, Y.H. Hou, and X. Chen, Microstructures and Fatigue Fracture Behavior of an Al-Cu-Mg-Ag Alloy with Addition of Rare Earth Er, *Mater. Sci. Eng. A*, 2010, **527**, p 1806–1814
6. B.M. Gable, G. Shiflet, and E. Starke, Jr., Alloy Development for the Enhanced Stability of Ω Precipitates in Al-Cu-Mg-Ag Alloys, *Metall. Mater. Trans. A*, 2006, **37**, p 1091–1105
7. R. Chester and I. Polmear, *The Metallurgy of Light Alloys*, Institution of Metallurgists, London, 1983, p 75
8. X.W. Zhou, Z.Y. Liu, S. Bai, M. Liu, and P.Y. Ying, The Influence of Various Ag Additions on the Nucleation and Thermal Stability of Omega Phase in Al-Cu-Mg Alloys, *Mater. Sci. Eng. A*, 2013, **564**, p 186–191
9. V.V. Teleshov, E.Y. Kaputkin, A.P. Golovleva, and N.P. Kosmacheva, Temperature Ranges of Phase Transformations and Mechanical Properties of Alloys of the Al-Cu-Mg-Ag System with Various Cu/Mg Ratios, *Met. Sci. Heat Treat.*, 2005, **47**, p 139–144
10. V. Teleshov, D. Andreev, and A. Golovleva, Effect of Chemical Composition on the Strength of Alloys of the Al-Cu-Mg-Ag System After Heating at 180-210 °C, *Met. Sci. Heat Treat.*, 2006, **48**, p 104–112
11. D.H. Xiao, J.N. Wang, D.Y. Ding, and S.P. Chen, Effect of Cu Content on the Mechanical Properties of an Al-Cu-Mg-Ag Alloy, *J. Alloys Compd.*, 2002, **343**, p 77–81
12. K. Ma, H. Wen, T. Hu, T.D. Topping, D. Isheim, D.N. Seidman, E.J. Lavernia, and J.M. Schoenung, Mechanical Behavior and Strengthening Mechanisms in Ultrafine Grain Precipitation-Strengthened Aluminum Alloy, *Acta Mater.*, 2014, **62**, p 141–155

13. D. Xiang, K.G. Liu, and B. Xu, Study Effect of Solution Treatment on Microstructures and Properties of 2014 Aluminium Alloy, *Light Alloy Fabr. Technol.*, 2005, **33**, p 44–47
14. S.H. Hong, K.H. Chung, and C.H. Lee, Effects of Hot Extrusion Parameters on the Tensile Properties and Microstructures of SiCw-2124Al Composites, *Mater. Sci. Eng. A*, 1996, **206**, p 225–232
15. S. Karabay, M. Yilmaz, and M. Zeren, Investigation of Extrusion Ratio Effect on Mechanical Behaviour of Extruded Alloy AA-6101 from the Billets Homogenised-Rapid Quenched and As-cast Conditions, *J. Mater. Process. Technol.*, 2005, **160**, p 138–147
16. X.Y. Liu, Q.L. Pan, Z.L. Lu, S.F. Cao, Y.B. He, and W.B. Li, Effects of Solution Treatment on the Microstructure and Mechanical Properties of Al-Cu-Mg-Ag Alloy, *Mater. Des.*, 2010, **31**, p 4392–4397
17. A. Rollett, F. Humphreys, G.S. Rohrer, and M. Hatherly, *Recrystallization and Related Annealing Phenomena*, Elsevier, Amsterdam, 2004
18. G.J. Zhang, G. Liu, X.D. Ding, J. Sun, and K.H. Chen, Experiment and Modeling Study of Aged Aluminium Alloys Strengthening Response, *Acta Metall. Sin.*, 2003, **39**, p 803–808
19. C.H. Chang, S.L. Lee, T.Y. Hsu, and J.C. Lin, Impact of Cu/Mg Ratio on Thermal Stability of Hot Extrusion of Al-4.6 Pct Cu-Mg-Ag Alloys, *Metall. Mater. Trans. A*, 2007, **38**, p 2832–2842
20. S. Bai, Z.Y. Liu, X.W. Zhou, P. Xia, and S.M. Zeng, Mg-Controlled Formation of Mg-Ag Co-clusters in Initial Aged Al-Cu-Mg-Ag Alloys, *J. Alloys Compd.*, 2014, **602**, p 193–198